

Ouyang Ziyuan, Jiang Jingshan, Li Chunlai, Sun Huixian, Zou Yongliao, Liu Jianzhong, Liu Jianjun, Zhao Baochang, Ren Xin, Yang Jianfeng, Zhang Wenxi, Wang Jianyu, Mou Lingli, Chang Jin, Zhang Liyan, Wang Huanyu, Li Yongquan, Zhang Xiaohui, Zheng Yongchun, Wang Shijin, Bian Wei. Preliminary scientific results of Chang'E-1 lunar orbiter: based on payloads detection data in the first phase. *Chin. J. Space Sci.*, 2008, **28**(5): 361~369

Preliminary Scientific Results of Chang'E-1 Lunar Orbiter: Based on Payloads Detection Data in the First Phase

OUYANG Ziyuan JIANG Jingshan LI Chunlai SUN Huixian
 ZOU Yongliao LIU Jianzhong LIU Jianjun ZHAO Baochang REN Xin
 YANG Jianfeng ZHANG Wenxi WANG Jianyu MOU Lingli CHANG Jin
 ZHANG Liyan WANG Huanyu LI Yongquan ZHANG Xiaohui
 ZHENG Yongchun WANG Shijin BIAN Wei

(*Chinese Academy of Sciences, Beijing 100864*)

Abstract Chang'E-1 lunar Orbiter was launched by Long March 3A rocket from Xichang Satellite Launch Center at 18:05 BT (Beijing Time) Oct. 24, 2007. It is the first step of its ambitious three-stage moon program, a new milestone in the Chinese space exploration history. The primary science objectives of Chang'E-1 lunar orbiter are to obtain three-Dimension (3D) stereo images of the lunar surface, to analyze the distribution and abundance of elements on the surface, to investigate the thickness of lunar soil, evaluate helium-3 resources and other characteristics, and to detect the space environment around the moon. To achieve the above four mission objectives, eight sets of scientific instruments are chosen as the payloads of the lunar orbiter, including a CCD stereo camera (CCD), a Sagnac-based interferometer spectrometer (IIM), a Laser Altimeter (LAM), a Microwave Radiometer (MRM), a Gamma-Ray Spectrometer (GRS), an X-ray spectrometer (XRS), a High-Energy Particle Detector (HPD), and two Solar Wind Ion Detectors (SWID). The detected data of the payloads show that all payloads work well. This paper introduces the status of payloads in the first phase and preliminary scientific results.

Key words Chang'E-1, Lunar orbiter, Payloads, Scientific results, China's Lunar Exploration Program

1 Introduction

China launched its first lunar orbiter, Chang'E-1, at 18:05 pm, of 24 October 2007, with a Long March 3A rocket from the No.3 launch tower in the Xichang Satellite Launch Center of southwestern Sichuan Province, China. On Nov. 27, 2007, Chinese government published the first image of moon of China's Lunar Exploration Program (CLEP), which was taken by the Chang'E-1.

Man-made satellites, manned space flights and conducting deep space exploration constitute a trilogy of space activities. Over the past 50 years, China has been able to launch man-made satellite with different sizes and shapes into earth orbit. It carried out manned space mission, and three Chinese astronauts were sent to space. The successful launch of Chang'E-1 is the first step of its ambitious three-stage moon program. It begins China's deep space exploration, and marks a new milestone in the Chinese

space exploration history. The primary technical objectives of the mission are: to develop and to launch China's first lunar orbiter, to validate the necessary lunar missions technology, to build a basic engineering system for lunar and future deep space exploration, and to explore the moon and gain experience for subsequent missions. The primary scientific objectives are to obtain 3-Dimension (3D) stereo images of the lunar surface, to analyze the distribution and abundance of major elements and minerals on the surface, to investigate the thickness of lunar regolith, to evaluate helium-3 resources and other characteristics, and to detect the space environment around the moon. To achieve the four scientific objectives, eight sets of scientific instruments are chosen as payloads of Chang'E-1 lunar orbiter. This paper introduced the status of payloads in the first month and preliminary scientific results.

2 Scientific Objectives and Payloads

There are four major scientific objectives of Chang'E-1 lunar orbiter.

The first objective is to draw pictures of the Moon and obtain 3D stereo images of the whole lunar surface. 3D stereo images are important materials to study the surface features of the moon. According to the image, the basic landforms, geological structures of the lunar surface could be divided, and outline graphs of lunar geology and structures could be made. The information also can provide reference for future soft landing places of CLEP^[1].

The second objective is to analyze the abundance and distribution of some elements on lunar surface remotely. The studied elements include K, Th, U, O, Si, Mg, Al, Ca, Te, Ti, Na, Mn, Cr, La, and etc. One Sagnac-based interferometer spectrometer, one gamma-ray spectrometer and one X-ray spectrometer are designed for this experiment. The information could be used to evaluate the abundance of some useful lunar resources.

The third objective is to measure the microwave Brightness Temperature (BT) of the lunar surface. Combining with other parameters, BT of the moon could be used to investigate properties of lunar regolith and to evaluate its depth, as well as the amount of helium-3 (${}^3\text{He}$) resources^[2]. A multi-channel microwave radiometer is designed for this experiment.

The forth objective is to orbit the space environment around the moon, to record data on the solar wind and to study the impact of solar activity on the earth and the moon. One high-energy particle detector and two solar wind ion detectors are designed for this objective.

To achieve the above four mission objectives, eight sets of scientific instruments are chosen as payloads of the lunar orbiter, including a CCD stereo camera (CCD), a Sagnac-based interferometer spectrometer (IIM), a Laser Altimeter (LAM), a Microwave Radiometer (MRM), a Gamma-Ray Spectrometer (GRS), an X-Ray Spectrometer (XRS), a High-energy Particle Detector (HPD), and two Solar Wind Ion Detectors (SWID) (see Table 1).

Table 1 Eight sets of scientific instruments aboard Chang'E-1 lunar orbiter

Payloads	Scientific objectives
three-line array CCD stereo camera	To map 3D stereo images of the lunar surface from 75°N to 75°S spatial resolution: 120 m swath width: 60 km
Sagnac-based interferometer spectrometer	To obtain the multi-spectral image of the lunar surface spatial resolution: 200 m band range: $\lambda = 0.48 \sim 0.96 \mu\text{m}$ swath width: 25.6 km
laser altimeter	To measure the altitude of the spacecraft from the nadir point of the lunar surface wavelength: 1064 nm laser emerged: 150 mJ resolution: 1 m
γ -ray spectrometer	To map the elemental abundances of the lunar surface energy range: 300 keV to 9 MeV energy resolution: 9% for ${}^{137}\text{Cs}$ at 662 keV

To be continued

Continued from previous page

X-ray spectrometer	To measure the flux and energy of X-rays emitted from lunar surface material and map the elemental abundances energy range: 0.5 to 60 keV resolution: 600 eV at 5.95 keV
microwave radiometer	To measure the microwave brightness temperature of the lunar surface and investigate characteristics of lunar regolith frequency channels: 3.0 GHz, 7.8 GHz, 19.35 GHz, 37 GHz brightness temperature sensitivity: 0.5 K
high-energy particle detector	To analyze the heavy ions and protons during the journey of Chang'E-1 from the Earth to the Moon and around the Moon. electrons: two energy level ($E_1 \geq 0.095$ MeV; $E_2 \geq 2.2$ MeV) protons: six energy level (P_1 : 4~8 MeV; P_2 : 8~14 MeV; P_3 : 14~26 MeV; P_4 : 26~60 MeV; P_5 : 60~150 MeV; P_6 : 150~400 MeV)
solar wind ion detectors	To measure the flux of solar wind ions during the journey of Chang'E-1 from the Earth to the Moon and around the Moon energy range: 0.05~20 keV

3 Preliminary Scientific Results of the Payloads

The CCD Stereo camera (CCD) is the principal payloads on Chang'E-1, and was first powered on in 20, Nov, 2007. Image data obtained by the CCD Stereo camera aboard Chang'E-1 lunar orbiter was successfully transmitted to Miyun and Kunming ground station. All of the eight sets of payloads were powered on and transmitted valid detection data till to 29, Nov, 2007.

3.1 CCD Stereo Camera

The three parallel rows of the plane CCD arrays can get the nadir, forward (17°), and backward (17°) view of the lunar surface. As the spacecraft moves forward, three two-dimension (2D) lunar surface maps will be acquired. After data processing, a 3D stereo image of the lunar surface could be obtained.

The first lunar image obtained by Chang'E-1 lunar orbiter was photographed by three-line array CCD stereo camera from the orbit height of about 200 km. Spatial resolution of the camera is about 120 m and swath width is 60 km.

The first lunar image is a composition of images from 19 orbits data acquired on Nov. 20 and Nov. 21, each of which covers a width of 60 kilometers of the lunar surface (Fig. 1). The image covers an area approximately 280 km wide and 460 km long, spanning 57° ~ 83° E longitude and 54° ~ 70° S latitude. The 60 km swath to the center right of the mosaic is the image that the CCD camera obtained from the

first orbit. The first image is part of the highland and is mainly composed of plagioclase. The image shows a rough lunar surface with scattered round craters of different sizes, shapes, structures and ages. The dark patch in the picture's upper right side shows the surface blanketed by basalt, a hard and dense volcanic rock.

After the first image, a typical rayed crater on the

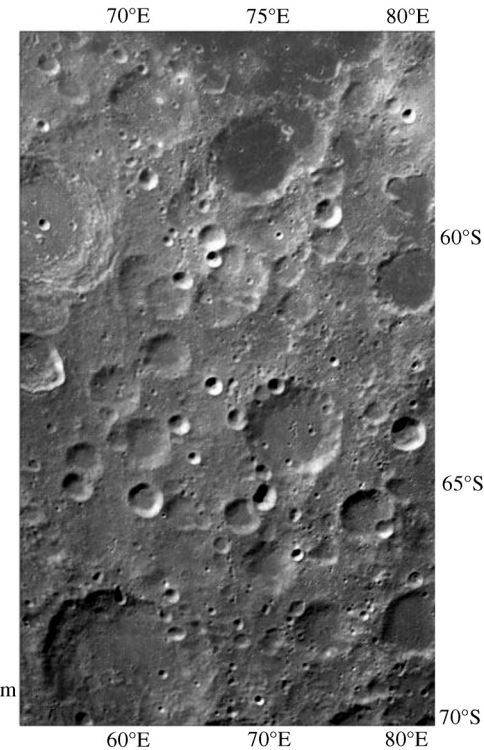


Fig.1 First lunar image obtained by Chang'E-1 lunar orbiter of China's Lunar Exploration Program

farside (Fig.2) and an image of polar region (Fig.3) were also published. The CCD camera works well at present. And the global 2D mosaic image of the Moon could be published in late 2008.

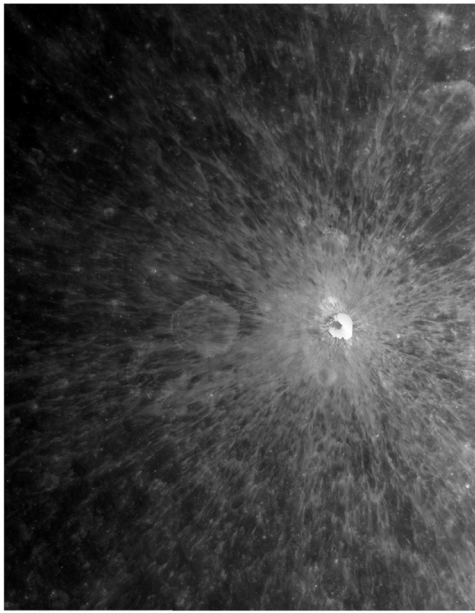


Fig.2 2D mosaic image of one typical rayed crater on the farside

3.2 Laser Altimeter

The task of Laser Altimeter (LAM) aboard the orbiter is to measure the altitude of the spacecraft from the nadir point of the lunar surface. 3D mosaic images could be obtained by combination of 2D image of CCD camera and altitude. Laser altimeter was powered on before dawn on Nov. 28, 2007. Till Dec. 31, 2007, 3 000 000 elevation data has been obtained by laser altimeter. Global Digital Elevation Model (DEM) was obtained based on elevation data (Fig. 4). The topography characteristics of the lunar surface can be identified from the DEM.

3.3 Sagnac-based Interferometer Spectrometer

The objective of Sagnac-based interferometer spectrometer (IIM) is to obtain the multi-spectral image of the lunar surface. From the image, the distribution

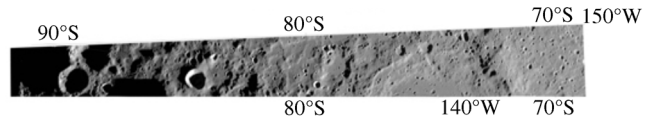


Fig.3 2D mosaic image of south polar region of the Moon

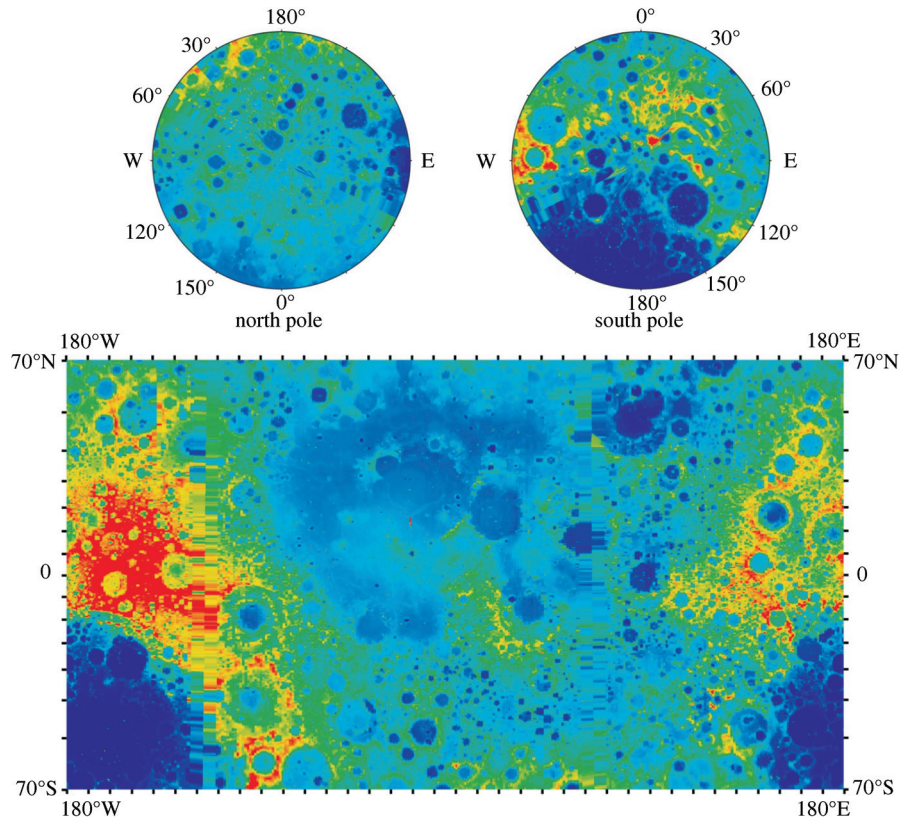


Fig.4 Global Digital Elevation Model (DEM) of the Moon

of major types of minerals and rocks could be identified. IIM was powered on at 22:45 BT, Nov. 26, 2007 (CST). The real time data was transmitted to Ground Segment for Data, Science, and Applications (GSDA) of China's Lunar Exploration Program. Fig. 5 is the preliminary results of Chang'E-1 Sagnac-based interferometer spectrometer. The results of spectral curve and image are consistent with ground calibration and verification test.

Relative errors of wavelength of IIM channels were listed in Table 2. Except Channel 1, 2, 3 and 32, average relative errors are between 2.5%~9.5%, which means the quality of the image is good.

3.4 Gamma-ray Spectrometer

The task of Gamma-Ray Spectrometer (GRS) is to measure the γ -ray radiated from the lunar surface and to map the elemental abundances of the lunar surface. The elements are U, Th, K, Fe, Ti, Si, O, Al, Mg, Ca, Na, Mn, Cr, REE (Gd).

GRS was powered on at 03:58 BT, Nov. 28, 2007 (CST), which is the last operated payload aboard on the orbiter. The preliminary results of GRS are presented in Tables 3 and 4. The abundances of K and U are similar with the results from Lunar Prospector.

3.5 X-ray Spectrometer

The task of X-ray spectrometer (XRS) is to measure

X-ray radiated from lunar surface materials, and to map the elemental abundances of Mg, Si, Al. XRS was powered on at 01:41 BT, Nov. 28, 2007 (CST). Preliminary results of XRS were presented in Fig. 6. Mg, Al, Si peak of Ka spectral line can be detected by four low-energy X-ray detectors. Data qualities can be improved after more detection data are accumulated.

3.6 Microwave Radiometer

The task of Microwave Radiometer (MRM) is to measure the brightness temperature of the lunar surface with a resolution of 0.5 K in four channels (3.0 GHz, 7.8 GHz, 19.35 GHz and 37 GHz). The brightness temperature of the moon is a function of complex dielectric constant, temperature, regolith thickness of lunar surface, and frequency and survey angle of the instrument. Combined with the physical properties of lunar surface materials, the lunar regolith thickness could be estimated. MRM was first powered on at 23:23 BT Nov. 27, 2007. The detection data of MRM was verified.

Brightness Temperature (BT) of the lunar surface during one orbital period is presented in Fig. 7. It shows that the brightness temperature is decreased with latitude during both lunar day and night. The results suggest that BT of lunar surface is mainly

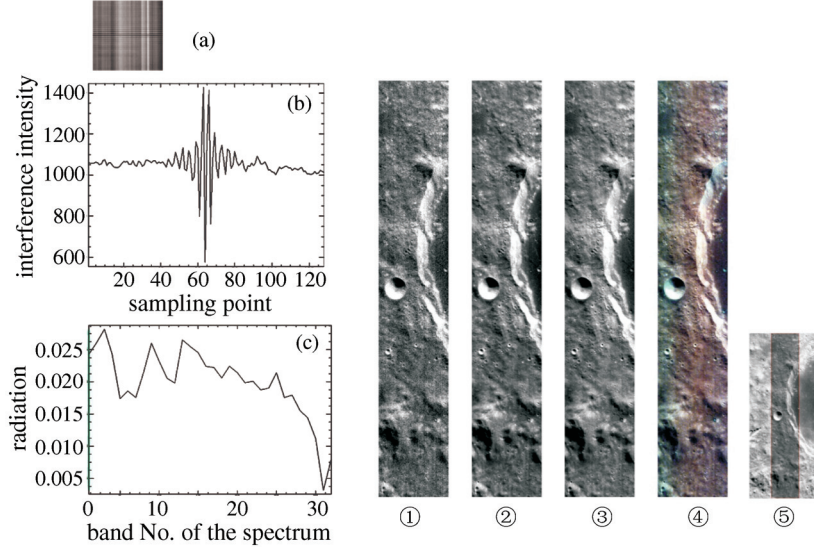


Fig.5 Preliminary results of Chang'E-1 Sagnac-based interferometer spectrometer. (a) Interferogram, (b) interferogram curve, (c) spectral curve. ① Spectral image of band No. 4 (Its center of wavelength is 504.96 nm), ② Spectral image of band No. 17 (Its center of wavelength is 644.64 nm), ③ Spectral image of band No. 30 (Its center of wavelength is 891.11 nm), ④ False color image from band No. 4, No. 17, No. 30, ⑤ Relative location of imaging area in the same orbit between image interferometer and CCD Stereo Camera

Table 2 Relative errors of wavelength of IIM channels

Channel	Wavelength /nm	relative error of wavelength/ (%)
1	480.91	23.22
2	488.67	13.83
3	496.68	11.85
4	504.96	8.20
5	513.52	6.37
6	522.37	5.16
7	531.54	6.00
8	541.03	5.49
9	550.87	4.95
10	561.07	3.88
11	571.65	3.57
12	582.65	3.59
13	594.07	3.95
14	605.95	3.06
15	618.32	2.64
16	631.2	2.36
17	644.63	2.46
18	658.64	2.47
19	673.28	2.37
20	688.58	2.34
21	704.6	2.30
22	721.37	2.51
23	738.97	2.22
24	757.44	2.48
25	776.86	2.17
26	797.31	1.86
27	818.85	2.00
28	841.6	1.97
29	865.65	1.90
30	891.11	1.87
31	918.11	4.38
32	946.8	19.26

influenced by solar irradiation. The influence is more obvious in low frequency than in high frequency. It means that BT of lunar surface in high frequency is mainly determined by surface thermal radiation. However, BT in low frequency is determined by combined contribution of surface and sub-surface thermal radiation.

3.7 High-energy Particle Detector

The task of High-energy Particle Detector (HPD) is to analyze the heavy ions and protons around the moon. The energy spectrum, component and flux of high-energy particle could be determined.

High-energy Particle Detector (HPD) was first powered on at 21:55 BT, Nov. 26, 2007. The work mode was continuous operation. Fig. 8 shows the counts from P_1 to P_6 energy channels when HDP was in the solar wind. Fig. 9 shows the counts of E_1 and E_2 energy channels when HDP was in the solar wind. Fig. 10 shows the counts of He, Li and C heavy ions when HDP was in the solar wind. All results indicate that the sun is quiet during the detection period. No solar proton event was observed.

3.8 Solar Wind Ion Detectors

The objective of Solar Wind Ion Detectors (SWID) is to measure the flux and energy spectrum of solar wind ions around the Moon. Some of the characteristics of SWID are as follows.

- Detected ions: solar wind ions and other low energy ions.
- Energy range: 0.05~20 keV.
- Energy channels: 48.
- Velocity: 150~2000 km/s.

Table 3 Abundance of K in Ocean Procellarum ($5^\circ \times 5^\circ$ /pixel) calculated from detection data of Chang'E-1 gamma-ray spectrometer

minimum latitude/(°)	maximal latitude/(°)	minimum longitude/(°)	maximal longitude/(°)	accumulated time/s	Chang'E-1 abundance/ppm.abundance/ppm	Lunar Prospector error	relative
12.5	17.5	-40	-35	1371	2237.25	2291.9	-0.023
12.5	17.5	0	5	1347	1205.75	1737.9	-0.306
12.5	17.5	40	45	1332	1008.15	787.03	0.280
22.5	27.5	-40	-35	1329	2131.71	1924.6	0.107
22.5	27.5	0	5	1341	2246.78	1992.6	0.127
22.5	27.5	40	45	1272	814.54	986.41	-0.174
32.5	37.5	-40	-35	1374	2151.01	1967.9	0.093
32.5	37.5	0	5	1482	3063.55	3011.5	0.017
32.5	37.5	40	45	1278	1102.45	923.99	0.193
47.5	52.5	-40	-35	1176	3392.84	2674.55	0.268
47.5	52.5	0	5	1272	2505.23	2023.8	0.237
47.5	52.5	40	45	1314	1308.44	1028.4	0.272

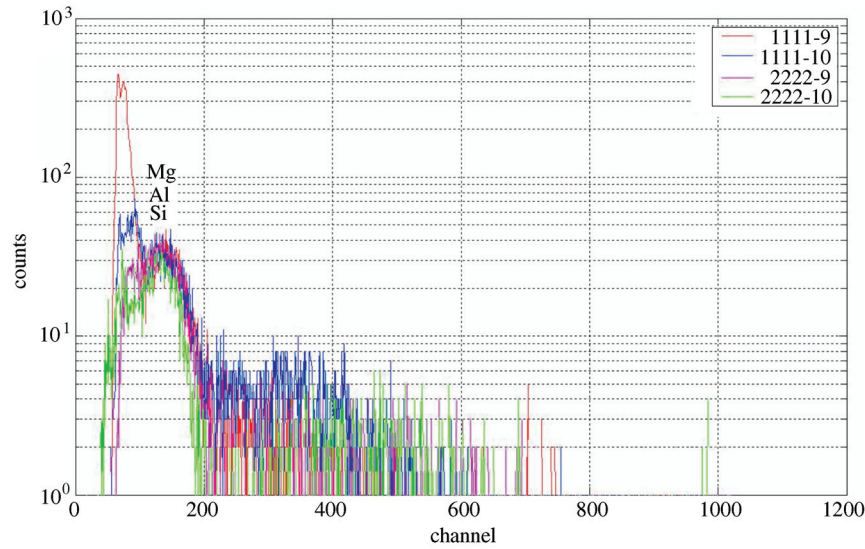


Fig.6 Mg, Al, Si peak of Ka spectral line detected by four low-energy X-ray detectors

Table 4 Abundance of U in Ocean Procellarum ($5^\circ \times 5^\circ/\text{pixel}$) calculated from detection data of Chang'E-1 gamma-ray spectrometer

minimum latitude/(°)	maximal longitude/(°)	minimum longitude/(°)	maximal longitude/(°)	accumulated time/s	Chang'E-1 abundance/ppm	Lunar Prospector abundance/ppm	relative error
12.5	17.5	-40	-35	1371	3.74	2.27	0.642
12.5	17.5	0	5	1347	1.97	1.69	0.164
12.5	17.5	40	45	1332	1.15	0.57	0.993
22.5	27.5	-40	-35	1329	2.48	1.77	0.400
22.5	27.5	0	5	1341	1.69	2.10	-0.197
22.5	27.5	40	45	1272	1.27	0.77	0.655
32.5	37.5	-40	-35	1374	2.73	2.23	0.221
32.5	37.5	0	5	1482	3.52	3.35	0.050
32.5	37.5	40	45	1278	1.31	0.72	0.823
47.5	52.5	-40	-35	1176	3.49	2.91	0.199
47.5	52.5	0	5	1272	2.84	1.96	0.449
47.5	52.5	40	45	1314	1.90	0.95	0.994

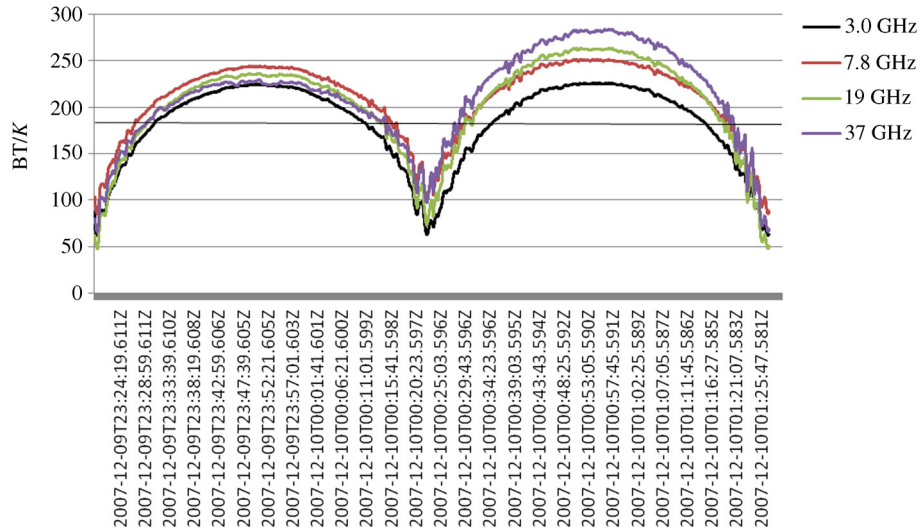


Fig.7 Brightness Temperature (BT) of the lunar surface during one orbital period

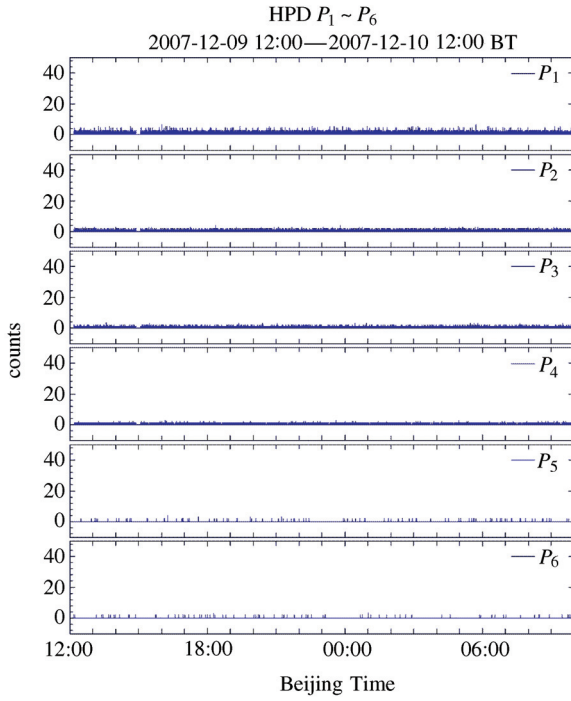


Fig.8 Measured results of P_1 to P_6 energy channels when HDP is surrounded by solar wind

SWID was first powered on Nov. 26, 2007. The work mode was continuous operation. The ACE satellite was located at the L1 libration point between the Earth and the Sun. Solar wind ion data could be provided by ACE. ACE could give the warning of geomagnetic activity in an hour's advance time. The results of SWID are similar with ACE measurement, which indicates that the detected data is reasonable and valid.

The moon was located between the sun and the Earth, and Chang'E-1 orbiter is in the solar wind on

Dec. 8 and 9, 2007. At that time, solar wind plasma was observed by SWID during quiet solar activity period. To ensure that the same plasma was detected by both ACE and Chang'E-1, we calculated the time delay from ACE to the moon based on the known distance from ACE to the moon and the velocity of solar wind plasma. The results of ACE and Chang'E-1 are all presented in Table 5. The consistency of ACE and Chang'E-1 proves that the data of SWID is valid. The difference between the two data is due to the different locations of ACE and Chang'E-1 orbiter.

Table 5 Comparison of solar wind plasma observed by ACE and SWID

Observe time	ACE	Chang'E-1 orbiter
16:30 BT, 2007-12-08	N_p	1.7
	V_p	297
	T	1.81×10^4
18:20 BT, 2007-12-08	N_p	1.8
	V_p	299
	T	1.58×10^4
18:00 BT, 2007-12-09	N_p	1.2
	V_p	330
	T	4.89×10^4
		3.83×10^4
		2.0
		275
		3.36×10^4
		1.6
		271
		1.2
		297
		6.53×10^4

4 Discussion and Conclusion

Preliminary scientific results of Chang'E-1 lunar orbiter were presented in the paper based on the data obtained in the first month. The results indicate that the eight sets of payloads of the lunar orbiter work well and the scientific data is valid. The future work could include:

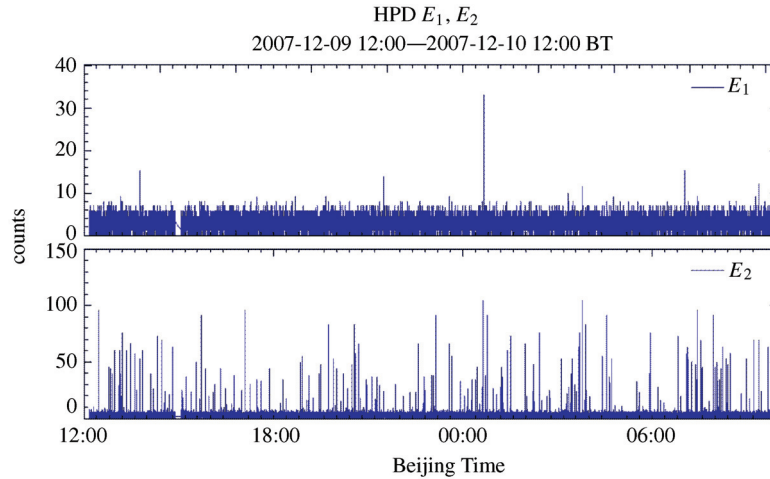


Fig.9 Measured results of E_1 and E_2 energy channels when HDP is surrounded by solar wind

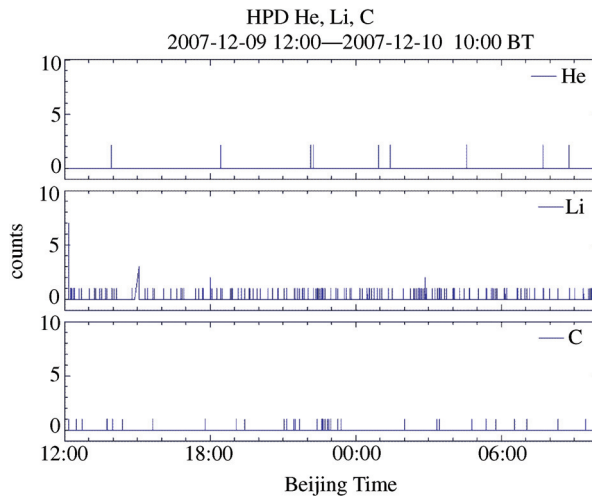


Fig.10 Measured results of He, Li and C heavy ions when HDP is surrounded by solar wind

(1) The CCD stereo camera has obtained 2D mosaic image data from 70°N to 70°S. Furthermore, the camera can also obtain image of the polar region. These mosaic images could provide more basic information for the study of lunar global topography.

(2) Laser altimeter has obtained 3 000 000 altitude data on the Moon. The data could supplement the lunar polar topography, and also contribute to the global 3D mosaic image.

(3) The results of Sagnac-based interferometer spectrometer suggest that, the uncertainty of most spectrums is lower than 15%, except in the minimum and maximum wavelengths.

(4) The results of gamma-ray spectrometer of Chang'E-1 orbiter were compared with Lunar

Prospector. The relative errors of K abundance and U are lower than 20% and 60% respectively. It was calculated based on the first month detection data. The precision of elemental abundance could be largely improved with the accumulation of detection data.

(5) The detection data of X-ray spectrometer accumulated in the first month was insufficient for the calculation of element abundance. Mg, Al, Si peak of Ka spectral line could be detected by four low-energy X-ray detectors.

(6) The brightness temperature of the lunar surface was measured by microwave radiometer. The results are valid and consistent with the observation of ground radio telescope. Based on the first measurement of global brightness temperature, some innovative results could be expected in the future.

(7) High-energy particle detector, and two solar wind detectors work well, and the results is consistent with the observations of other satellites. The data is useful for the study of space environment between the moon and the Earth.

References

- [1] Ouyang Ziyuan. Introduction to Lunar Sciences. Beijing: China Astronautics Publishing House, 2005
- [2] Zheng Yongchun. Development of Lunar soil simulants and characteristics of microwave radiation of lunar regolith. In: Ph.D Thesis Graduate University of Chinese Academy of Sciences, 2005
- [3] Zheng Yongchun *et al.* Implanted helium-3 abundance distribution on the moon. In: 39th Lunar and Planetary Science Conference, League Texas, 2008